

Research Article

Convergence Analysis of Two Parallel Methods for Common Variational Inclusion Problems Involving Demicontractive Mappings

Thanasak Mouktonglang,^{1,2} Kanyuta Pochinapan,^{1,2} Pariwate Varnakovida,^{3,4} Raweerote Suparatulorn ⁵ and Sompop Moonchai^{1,2}

¹Advanced Research Center for Computational Simulation, Chiang Mai University, Chiang Mai 50200, Thailand

²Department of Mathematics, Faculty of Science, Chiang Mai University, Chiang Mai 50200, Thailand

³KMUTT Geospatial Engineering and Innovation Center, Faculty of Science, King Mongkut's University of Technology Thonburi, Thung Khru, Bangkok 10140, Thailand

⁴Department of Mathematics, Faculty of Science, King Mongkut's University of Technology Thonburi, Thung Khru, Bangkok 10140, Thailand

⁵Elementary Education Program, Faculty of Education, Suan Dusit University Lampang Center, Lampang 52100, Thailand

Correspondence should be addressed to Raweerote Suparatulorn; raweerote.s@gmail.com

Received 22 September 2022; Revised 16 January 2023; Accepted 6 April 2023; Published 30 May 2023

Academic Editor: Mohammad W. Alomari

Copyright © 2023 Thanasak Mouktonglang et al. This is an open access article distributed under the Creative Commons Attribution License, which permits unrestricted use, distribution, and reproduction in any medium, provided the original work is properly cited.

The main objective of this article is to propose two novel parallel methods for solving common variational inclusion and common fixed point problems in a real Hilbert space. Strong convergence theorems of both methods are established by allowing for some mild conditions. Moreover, numerical studies of the signal recovery problem consisting of various blurred filters demonstrate the computational behavior of the proposed methods and other existing methods.

1. Introduction

Throughout this article, a real Hilbert space is denoted by \mathcal{H} with inner product $\langle \cdot, \cdot \rangle$ and associated norm $\|\cdot\|$. It is defined that $[K] := \{1, 2, \dots, K\}$ is the index set for any positive integer K . Let \mathbb{R} and \mathbb{N} be the sets of real numbers and nonnegative integers, respectively. The problem of identifying a point $v \in \mathcal{H}$ such that

$$0 \in (F_i + G_i)v, \quad (1)$$

is called the common variational inclusion problem (CVIP), where $F_i: \mathcal{H} \rightarrow \mathcal{H}$ is a single valued mapping and $G_i: \mathcal{H} \rightarrow 2^{\mathcal{H}}$ is a multivalued mapping for all $i \in [K]$. If $[K] = \{1\}$, then the CVIP (1) becomes the variational inclusion problem (VIP). The VIP is widely acknowledged as a fundamental aspect of nonlinear analysis, and it plays a pivotal role in numerous mathematical models, such as

composite minimization problems, variational inequality problems, split feasibility problems, and convex programming. Its broad range of applications extends to various areas, including machine learning, signal and image recovery, and beyond (see [1–7]). To solve the VIP, several splitting algorithms have been created and refined; one of the most prominent splitting algorithms is the forward-backward splitting method (see [8, 9] for more information). Chen and Rockafellar [10] used this method in 1997 to obtain a weak convergence result. Later, Tseng [11] created a modification of the forward-backward splitting method, known as the forward-backward-forward method or Tseng's method. This approach makes use of an adaptive line-search rule and relaxes the assumptions of [10] in order to prove weak convergence. In 1964, Polyak [12] introduced the inertial extrapolation technique as a means to expedite the convergence of iterative algorithms, commonly known

as the heavy ball method. This powerful optimization algorithm has since demonstrated its efficacy in accelerating the rate of convergence of the classical gradient descent method and found applications in various fields, such as machine learning, computer vision, and control theory. Padcharoen et al. [13] recently presented a splitting method for solving the VIP in \mathcal{H} , which was developed from Tseng's method with the inertial extrapolation technique. Weak convergence of this method was established under usual assumptions. This method also solved the problems of image deblurring and image recovery. Some recent results for the VIP and related problems are stated in the studies of [14–25]. In order to solve the VIP when both the operators are multivalued maximal monotone mappings, two of the most often used splitting algorithms include the Peaceman–Rachford splitting algorithm [26] and the Douglas–Rachford splitting algorithm [27]. These splitting algorithms have been extensively studied, see [28–30].

In many practical situations, it is necessary to identify a solution that satisfies multiple constraints. Such constraints can be expressed in terms of a nonlinear functional model. In this paper, our focus is on the investigation of common variational inclusion and common fixed point problems. The motivation for this study arises from their potential utility in addressing real-world challenges, such as signal and image recovery problems, wherein a diverse set of blur filters may be present, see [31, 32]. Furthermore, in Section 4, we demonstrate the applicability of our proposed method in solving signal recovery problems using a variety of blurred filters. This problem consists of finding a point $\bar{x} \in \mathcal{H}$ such that

$$0 \in (F_i + G_i)\bar{x} \text{ and } \bar{x} = S_i\bar{x}, \quad (2)$$

where $G_i: \mathcal{H} \rightarrow 2^{\mathcal{H}}$ is a multivalued mapping and F_i, S_i are single valued mappings on \mathcal{H} for all $i \in [K]$. Suantai et al. [31] proposed a parallel algorithm based on the shrinking projection method of a finite family of G -nonexpansive mappings in \mathcal{H} with directed graphs to identify a common fixed point. This approach has been applied to solve signal recovery problems in scenarios where the noise type is unknown. Similarly, Suparatulatorn and Chaichana [32] investigated the problem of image recovery using CVIP (1) as the mathematical model, specifically for multiple blurred filters. Chang et al. [33] introduced an algorithm based on the viscosity approximating scheme to obtain strong convergence for solving CVIP in a uniformly convex and q -uniformly smooth Banach space. In a recent study, Mouktonglang et al. [34] proposed a parallel algorithm that utilizes the inertial Mann iteration process to demonstrate a weak convergence result for solving problem (2) subject to certain control conditions in \mathcal{H} . Numerous intriguing findings have been reported in the literature concerning problem (2) and related problems. For further details, see [35–39].

Motivated by these results, we develop two parallel algorithms based on Tseng's method, the viscosity approximating scheme, and the inertial extrapolation technique for solving the problem (2) in \mathcal{H} . Strong convergence results of

the proposed methods are provided under standard and mild conditions. As applications, we apply our algorithms in order to solve the signal recovery problem using a variety of blurred filters.

2. Preliminaries

We refer to \rightharpoonup and \longrightarrow , respectively, as weak and strong convergence. We then gather the definitions and lemmas required to support our key results. Let C be a nonempty, closed, and convex subset of a real Hilbert space \mathcal{H} . The metric projection P_C from \mathcal{H} onto C is defined by the following equation:

$$P_C z := \arg \min_{w \in C} \|z - w\|, \quad (3)$$

for all $z \in \mathcal{H}$. From this definition, it follows that

$$\langle z - P_C z, w - P_C z \rangle \leq 0, \quad (4)$$

for any $z \in \mathcal{H}$ and $w \in C$. It is important to mention that the following equalities and inequality hold true in inner product spaces. Assume $z, w \in \mathcal{H}$,

$$\|z + w\|^2 = \|z\|^2 + 2\langle z, w \rangle + \|w\|^2, \quad (5)$$

$$\|z + w\|^2 \leq \|z\|^2 + 2\langle w, z + w \rangle, \quad (6)$$

$$\|az + (1 - a)w\|^2 = a\|z\|^2 + (1 - a)\|w\|^2 - a(1 - a)\|z - w\|^2, \quad (7)$$

for any $a \in \mathbb{R}$. Assume that $G: \mathcal{H} \rightarrow 2^{\mathcal{H}}$ is a multivalued mapping and $S: \mathcal{H} \rightarrow \mathcal{H}$ is a self-mapping.

Definition 1. S is considered to be

- (i) \mathcal{L} -Lipschitz continuous if there is $\mathcal{L} > 0$ such that for all $z, w \in \mathcal{H}$,

$$\|Sz - Sw\| \leq \mathcal{L}\|z - w\|. \quad (8)$$

- (ii) nonexpansive if S is 1-Lipschitz continuous,
- (iii) μ -demicontractive [40, 41] if $\text{Fix}(S) \neq \emptyset$ and there is $\mu \in (0, 1)$ such that for all $p \in \text{Fix}(S)$ and all $z \in \mathcal{H}$,

$$\|Sz - p\|^2 \leq \|z - p\|^2 + \mu\|z - Sz\|^2. \quad (9)$$

Definition 2. G is considered to be

- (i) monotone if for all $(x, z), (y, w) \in \text{graph}(G)$ (the graph of mapping G), $\langle z - w, x - y \rangle \geq 0$,
- (ii) maximal monotone if for every $(x, z) \in \mathcal{H} \times \mathcal{H}$, $\langle z - w, x - y \rangle \geq 0$ for all $(y, w) \in \text{graph}(G)$ if and only if $(x, z) \in \text{graph}(G)$.

Definition 3 (See [42]). Suppose that $\text{Fix}(S) \neq \emptyset$. Then, $I - S$ is considered to be demiclosed at zero if for any $\{v_k\} \subset \mathcal{H}$, the following statement is valid:

$$(I - S)v_k \longrightarrow 0 \text{ and } v_k \rightharpoonup \bar{v} \implies \bar{v} \in \text{Fix}(S). \quad (10)$$

Lemma 4 (See [43]). $S + G$ is maximal monotone mapping, where S is a Lipschitz continuous and monotone mapping, and G is a maximal monotone mapping.

Lemma 5 (See [44]). Let G be a maximal monotone mapping. If $T_\gamma := (I + \gamma G)^{-1}(I - \gamma S)$ and $\gamma > 0$, then $\text{Fix}(T_\gamma) = (S + G)^{-1}(0)$.

Lemma 6 (See [45]). Suppose that S is a μ -demicontractive mapping with $\text{Fix}(S) \neq \emptyset$ and let $S_\alpha = \alpha I + (1 - \alpha)S$, where $\alpha \in (\mu, 1)$. Then $\|S_\alpha z - p\|^2 \leq \|z - p\|^2 - (1 - \alpha)(\alpha - \mu)\|Sz - z\|^2$ for all $p \in \text{Fix}(S)$ and all $z \in \mathcal{H}$.

Lemma 7 (See [46]). Let $\{b_k\}$ denote a sequence of real numbers such that $\limsup_{k \rightarrow \infty} b_k \leq 0$, and let $\{a_k\}$ and $\{c_k\}$ be nonnegative sequences of real numbers such that $\sum_{k=1}^{\infty} c_k < \infty$. If for any $k \in \mathbb{N}$ such that

$$a_{k+1} \leq (1 - \gamma_k)a_k + \gamma_k b_k + c_k, \quad (11)$$

where $\{\gamma_k\}$ is a sequence in $(0, 1)$ such that $\sum_{k=1}^{\infty} \gamma_k = \infty$, then $\lim_{k \rightarrow \infty} a_k = 0$.

Lemma 8. (See [47]) Let $\{\Gamma_k\}$ denote a sequence of real numbers such that there exists a subsequence $\{\Gamma_{k_q}\}_{q \in \mathbb{N}}$ of $\{\Gamma_k\}$ satisfying $\Gamma_{k_q} < \Gamma_{k_q+1}$ for all $q \in \mathbb{N}$. Suppose $\{\psi(k)\}_{k \geq k^*}$ is a sequence of integers defined by

$$\psi(k) := \max\{n \leq k: \Gamma_n < \Gamma_{n+1}\}. \quad (12)$$

Then, $\{\psi(k)\}_{k \geq k^*}$ is a nondecreasing sequence such that $\lim_{k \rightarrow \infty} \psi(k) = \infty$, and for all $k \geq k^*$, we have that $\Gamma_{\psi(k)} \leq \Gamma_{\psi(k)+1}$ and $\Gamma_k \leq \Gamma_{\psi(k)+1}$.

3. Convergence Analysis

This section aims at presenting Algorithms 1 and 2 for coping with the problem (2). Let us begin by introducing some assumptions that will be required for the ensuing convergence analysis, for all $i \in [K]$.

Assumption 9. $F_i: \mathcal{H} \rightarrow \mathcal{H}$ is \mathcal{L}_i -Lipschitz continuous and monotone mapping.

Assumption 10. $G_i: \mathcal{H} \rightarrow 2^{\mathcal{H}}$ is maximal monotone mapping.

Assumption 11. $S_i: \mathcal{H} \rightarrow \mathcal{H}$ is μ_i -demicontractive mapping and $\phi: \mathcal{H} \rightarrow \mathbb{R}$ is a differentiable function.

Assumption 12. $\Psi := \cap_{i \in [K]} (F_i + G_i)^{-1}(0) \cap \cap_{i \in [K]} \text{Fix}(S_i)$ is nonempty.

Assumption 13. $\{\theta_k\} \subset (0, 1)$, $\{\xi_k\} \subset (0, \infty)$ and $\{\alpha_k^i\} \subset (\mu_i, \bar{\alpha}_i) \subset (0, 1)$, for some $\bar{\alpha}_i > 0$.

Assumption 14. $\{\tau_k^i\} \subset [\tau_i, \bar{\tau}_i] \subset (0, 1/\mathcal{L}_i)$, for some $\tau_i, \bar{\tau}_i > 0$.

Assumption 15. $I - S_i$ is demiclosed at zero.

Assumption 16. $\lim_{k \rightarrow \infty} \theta_k = \lim_{k \rightarrow \infty} \xi_k/\theta_k \|v_k - v_{k-1}\| = 0$, $\sum_{k=1}^{\infty} \theta_k = \infty$ and $\Phi := \nabla \phi$ is contraction with constant $\rho \in (0, 1)$, where $\{v_k\}$ is defined in Algorithms 1 and 2.

Lemma 17. Let $S_i: \mathcal{H} \rightarrow \mathcal{H}$ be a mapping and $F_i: \mathcal{H} \rightarrow \mathcal{H}$ be a \mathcal{L}_i -Lipschitz continuous mapping for all $i \in [K]$. If Assumption 10 holds, $\tau_k^i > 0$ and $\rho_k = h_k^i = S_i j_k^i$ for all $i \in [K]$ in Algorithms 1, then $\rho_k \in \Psi$.

Proof. From $\rho_k = h_k^i$, we have that, for all $i \in [K]$,

$$\rho_k = (I + \tau_k^i G_i)^{-1} (I - \tau_k^i F_i) \rho_k. \quad (13)$$

Using Lemma 5, we get that $\rho_k \in \cap_{i \in [K]} (F_i + G_i)^{-1}(0)$. Because of the Lipschitz condition of F_i , it is evident that, for all $i \in [K]$,

$$\|h_k^i - j_k^i\| \leq \tau_k^i \mathcal{L}_i \|\rho_k - h_k^i\|. \quad (14)$$

Since $\tau_k^i \mathcal{L}_i > 0$ and $\rho_k = h_k^i$, it follows that $h_k^i = j_k^i$ and so $\rho_k = h_k^i = j_k^i = S_i j_k^i$ for all $i \in [K]$. That is, $\rho_k \in \cap_{i \in [K]} \text{Fix}(S_i)$. Therefore, $\rho_k \in \Psi$. \square

Lemma 18. Assume that Assumptions 9–14 are satisfied. Then, we have

$$\|u_k^i - v\|^2 + (1 - \alpha_k^i)(\alpha_k^i - \mu_i) \|S_i j_k^i - j_k^i\|^2 + [1 - (\bar{\tau}_i \mathcal{L}_i)^2] \|\rho_k - h_k^i\|^2 \leq \|\rho_k - v\|^2, \quad (15)$$

$$\|j_k^i - \rho_k\| \leq (1 + \bar{\tau}_i \mathcal{L}_i) \|\rho_k - h_k^i\|, \quad (16)$$

Initialization: Select arbitrary elements $v_0, v_1 \in \mathcal{H}$ and set $k := 1$.
Iterative Steps: Create $\{v_k\}$ through the following process:
Step 1. Set
 $\rho_k = v_k + \theta_k (\Phi(v_k) - v_k) + \xi_k (v_k - v_{k-1})$
and calculate, for all $i \in [K]$,
 $h_k^i = (I + \tau_k^i G_i)^{-1} (I - \tau_k^i F_i) \rho_k$.
Step 2. Compute, for all $i \in [K]$,
 $j_k^i = h_k^i - \tau_k^i (F_i h_k^i - F_i \rho_k)$ and $u_k^i = S_i j_k^i - \alpha_k^i (S_i j_k^i - j_k^i)$.
If $\rho_k = h_k^i = S_i j_k^i$ for all $i \in [K]$, then stop and $\rho_k \in \Psi$. Otherwise, go to **Step 3**.
Step 3. Evaluate
 $v_{k+1} = \operatorname{argmax}\{\|u_k^i - \rho_k\| : i \in [K]\}$.
Replace k by $k + 1$ and go back to **Step 1**.

ALGORITHM 1: Inertial Tseng Mann parallel algorithm 1.

for all $v \in \Psi$ and $i \in [K]$.

Proof. Let $v \in \Psi$. Using (5) with the conditions of τ_k^i and F_i , it follows that, for all $i \in [K]$,

$$\begin{aligned} \|j_k^i - v\|^2 &= \|h_k^i - v\|^2 - 2\tau_k^i \langle h_k^i - v, F_i h_k^i - F_i \rho_k \rangle + (\tau_k^i)^2 \|F_i h_k^i - F_i \rho_k\|^2 \\ &= \|h_k^i - \rho_k\|^2 - 2\langle h_k^i - \rho_k, h_k^i - \rho_k \rangle + 2\langle h_k^i - \rho_k, h_k^i - v \rangle + \|\rho_k - v\|^2 \\ &\quad - 2\tau_k^i \langle h_k^i - v, F_i h_k^i - F_i \rho_k \rangle + (\bar{\tau}_i \mathcal{L}_i)^2 \|h_k^i - \rho_k\|^2 \\ &\leq \|\rho_k - v\|^2 - [1 - (\bar{\tau}_i \mathcal{L}_i)^2] \|\rho_k - h_k^i\|^2 - 2\langle h_k^i - v, \rho_k - h_k^i - \tau_k^i (F_i \rho_k - F_i h_k^i) \rangle. \end{aligned} \quad (17)$$

The definition of h_k^i implies that for all $i \in [K]$,

$$(I - \tau_k^i F_i) \rho_k \in (I + \tau_k^i G_i) h_k^i. \quad (18)$$

This implies that there is $g_k^i \in G_i h_k^i$ such that

$$g_k^i = \frac{1}{\tau_k^i} (\rho_k - h_k^i - \tau_k^i F_i \rho_k), \quad (19)$$

for all $i \in [K]$. The maximally monotonic nature of $F_i + G_i$ leads us to the conclusion that for all $i \in [K]$,

$$\langle F_i h_k^i + g_k^i, h_k^i - v \rangle \geq 0, \quad (20)$$

implying that for all $i \in [K]$,

$$\langle h_k^i - v, \rho_k - h_k^i - \tau_k^i (F_i \rho_k - F_i h_k^i) \rangle \geq 0. \quad (21)$$

This combined with (17) yields that for all $i \in [K]$,

$$\|j_k^i - v\|^2 \leq \|\rho_k - v\|^2 - [1 - (\bar{\tau}_i \mathcal{L}_i)^2] \|\rho_k - h_k^i\|^2. \quad (22)$$

This follows from Lemma 6 that for all $i \in [K]$,

$$\begin{aligned} \|u_k^i - v\|^2 &\leq \|j_k^i - v\|^2 - (1 - \alpha_k^i) (\alpha_k^i - \mu_i) \|S_i j_k^i - j_k^i\|^2 \\ &\leq \|\rho_k - v\|^2 - [1 - (\bar{\tau}_i \mathcal{L}_i)^2] \|\rho_k - h_k^i\|^2 - (1 - \alpha_k^i) (\alpha_k^i - \mu_i) \|S_i j_k^i - j_k^i\|^2. \end{aligned} \quad (23)$$

Furthermore, using the inequality (14) with the condition of τ_k^i and triangle inequality, we derive that inequality (16) is true. \square

Lemma 19. Assume that Assumptions 9–15 hold. If there is a subsequence $\{\rho_{k_m}\}$ of $\{\rho_k\}$ such that $\rho_{k_m} \rightarrow \bar{r} \in \mathcal{H}$ and $\lim_{m \rightarrow \infty} \|\rho_{k_m} - h_{k_m}^i\| = \lim_{m \rightarrow \infty} \|S_i j_{k_m}^i - j_{k_m}^i\| = 0$ for all $i \in [K]$. Then, $\bar{r} \in \Psi$.

Proof. Applying the inequality (16) with $\lim_{m \rightarrow \infty} \|\rho_{k_m} - h_{k_m}^i\| = 0$ for all $i \in [K]$, we get that $\lim_{m \rightarrow \infty} \|\rho_{k_m} - j_{k_m}^i\| = 0$ for all $i \in [K]$. It follows that $j_{k_m}^i \rightarrow \bar{r}$ for all $i \in [K]$, which together with $\lim_{m \rightarrow \infty} \|S_i j_{k_m}^i - j_{k_m}^i\| = 0$ and Assumption 15 indicates that $\bar{r} \in \bigcap_{i \in [K]} \operatorname{Fix}(S_i)$. Next, we exhibit $\bar{r} \in \bigcap_{i \in [K]} (F_i + G_i)^{-1}(0)$. For all $i \in [K]$, let $(v_i, u_i) \in \operatorname{graph}(F_i + G_i)$ be equivalent to $u_i - F_i v_i \in G_i v_i$. This implies, based on the definition of h_k^i , that $1/\tau_{k_m}^i (\rho_{k_m} -$

$h_{k_m}^i - \tau_{k_m}^i F_i \rho_{k_m} \in G_i h_{k_m}^i$ for all $i \in [K]$. By the maximal monotonicity of G_i , we have that, for all $i \in [K]$,

$$\langle v_i - h_{k_m}^i, u_i - F_i v_i - \frac{1}{\tau_{k_m}^i} (\rho_{k_m} - h_{k_m}^i - \tau_{k_m}^i F_i \rho_{k_m}) \rangle \geq 0. \quad (24)$$

So, for all $i \in [K]$,

$$\begin{aligned} \langle v_i - h_{k_m}^i, u_i \rangle &\geq \langle v_i - h_{k_m}^i, F_i v_i + \frac{1}{\tau_{k_m}^i} (\rho_{k_m} - h_{k_m}^i - \tau_{k_m}^i F_i \rho_{k_m}) \rangle \\ &= \langle v_i - h_{k_m}^i, F_i v_i - F_i h_{k_m}^i \rangle + \langle v_i - h_{k_m}^i, F_i h_{k_m}^i - F_i \rho_{k_m} \rangle \\ &\quad + \frac{1}{\tau_{k_m}^i} \langle v_i - h_{k_m}^i, \rho_{k_m} - h_{k_m}^i \rangle \\ &\geq \langle v_i - h_{k_m}^i, F_i h_{k_m}^i - F_i \rho_{k_m} \rangle + \frac{1}{\tau_{k_m}^i} \langle v_i - h_{k_m}^i, \rho_{k_m} - h_{k_m}^i \rangle. \end{aligned} \quad (25)$$

This can be deduced from the Lipschitz continuity of F_i , $\lim_{m \rightarrow \infty} \|\rho_{k_m} - h_{k_m}^i\| = 0$ and $\tau_{k_m}^i \in [\tau_i, \bar{\tau}_i]$ that

$$\langle v_i - \bar{\tau}, u_i \rangle = \lim_{m \rightarrow \infty} \langle v_i - h_{k_m}^i, u_i \rangle \geq 0, \quad (26)$$

For all $i \in [K]$, when considered together with the maximal monotonicity of $F_i + G_i$, leads to the conclusion that $0 \in (F_i + G_i) \bar{\tau}$ for all $i \in [K]$, is equivalent to $\bar{\tau} \in \bigcap_{i \in [K]} (F_i + G_i)^{-1}(0)$. As a result, $\bar{\tau} \in \Psi$. \square

Theorem 20. *If Assumptions 9–16 hold, then the sequence $\{v_k\}$ generated by Algorithms 1 converges strongly to $v := (P_\Psi \circ \Phi)v$.*

Proof. Let $p \in \Psi$. From $\lim_{k \rightarrow \infty} \xi_k / \theta_k \|v_k - v_{k-1}\| = 0$, we obtain the following equation:

$$\xi_k \|v_k - v_{k-1}\| \leq \theta_k R_1, \quad (27)$$

for some $R_1 > 0$. Since Φ is contraction with constant $\rho \in [0, 1)$ and using (27), we have to compute the following expression:

$$\begin{aligned} \|\rho_k - p\| &= \|v_k + \theta_k (\Phi(v_k) - v_k) + \xi_k (v_k - v_{k-1}) - p\| \\ &\leq \theta_k \|\Phi(v_k) - p\| + (1 - \theta_k) \|v_k - p\| + \xi_k \|v_k - v_{k-1}\| \\ &\leq \theta_k \|\Phi(v_k) - \Phi(p)\| + \theta_k (\|\Phi(p) - p\| + R_1) + (1 - \theta_k) \|v_k - p\| \\ &\leq (1 - \gamma_k) \|v_k - p\| + \gamma_k R_2 \\ &\leq \max \{ \|v_k - p\|, R_2 \}, \end{aligned} \quad (28)$$

where $\gamma_k = \theta_k (1 - \rho)$ and $R_2 = \|\Phi(p) - p\| + R_1 / (1 - \rho)$. Using the inequality (15) with the definition of v_{k+1} and Assumptions 13 and 14 implies that

$$\|v_{k+1} - p\| \leq \|\rho_k - p\|. \quad (29)$$

Therefore, we can conclude that $\|v_{k+1} - p\| \leq \max \{ \|v_k - p\|, R_2 \}$ for any $k \in \mathbb{N}$. Consequently, $\{v_k\}$ is bounded sequence. Moreover, the sequence $\{\Phi(v_k)\}$ is bounded. Since the set Ψ is nonempty, closed and convex, there is a unique $v \in \Psi$ such that $v = (P_\Psi \circ \Phi)v$. By (4), we also get that for any $y \in \Psi$,

$$\langle \Phi(v) - v, y - v \rangle \leq 0. \quad (30)$$

Now, for each $k \in \mathbb{N}$, set $\Xi_k := \|v_k - v\|^2$. Applying (28), we have the following equation:

$$\begin{aligned} \|\rho_k - v\|^2 &\leq ((1 - \gamma_k) \|v_k - v\| + \gamma_k R_2)^2 \\ &= (1 - \gamma_k)^2 \Xi_k + \gamma_k (2R_2 (1 - \gamma_k) \|v_k - v\| + \gamma_k R_2^2) \\ &\leq \Xi_k + \gamma_k R_3, \end{aligned} \quad (31)$$

for some $R_3 > 0$. This follows from (15) that

Initialization: Let $v_0, v_1 \in \mathcal{H}$, $\lambda_i > 0$ and $\tau_1^i \in (0, 1/\mathcal{L}_i)$ for all $i \in [K]$, and set $k := 1$.

Iterative Steps: Create $\{v_k\}$ through the following process:

Step 1. Set

$$\rho_k = v_k + \theta_k (\Phi(v_k) - v_k) + \xi_k (v_k - v_{k-1})$$

and calculate, for all $i \in [K]$,

$$h_k^i = (I + \tau_k^i G_i)^{-1} (I - \tau_k^i F_i) \rho_k.$$

Step 2. Compute, for all $i \in [K]$,

$$j_k^i = h_k^i - \tau_k^i (F_i h_k^i - F_i \rho_k) \text{ and } u_k^i = S_i j_k^i - \alpha_k^i (S_i j_k^i - j_k^i).$$

If $\rho_k = h_k^i = S_i j_k^i$ for all $i \in [K]$, then stop and $\rho_k \in \Psi$. Otherwise, go to **Step 3**.

Step 3. Evaluate

$$v_{k+1} = \operatorname{argmax}\{\|u_k^i - \rho_k\| : i \in [K]\}$$

and update, for all $i \in [K]$,

$$\tau_{k+1}^i = \begin{cases} \min\{\lambda_i \|\rho_k - h_k^i\| / \|F_i \rho_k - F_i h_k^i\|, \tau_k^i\}, & \text{if } F_i \rho_k \neq F_i h_k^i, \\ \tau_k^i & \text{otherwise.} \end{cases}$$

Replace k by $k + 1$ and go back to **Step 1**.

ALGORITHM 2: Inertial Tseng Mann parallel algorithm 2.

$$\begin{aligned} (1 - \alpha_k^i)(\alpha_k^i - \mu_i) \|S_i j_k^i - j_k^i\|^2 \\ + [1 - (\bar{\tau}_i \mathcal{L}_i)^2] \|\rho_k - h_k^i\|^2 \leq \Xi_k - \|u_k^i - v\|^2 + \gamma_k R_3. \end{aligned} \quad (32)$$

For all $i \in [K]$. It implies by (32) that there is $i_k \in [K]$ such that

$$(1 - \alpha_k^{i_k})(\alpha_k^{i_k} - \mu_{i_k}) \|S_{i_k} j_k^{i_k} - j_k^{i_k}\|^2 + [1 - (\bar{\tau}_{i_k} \mathcal{L}_{i_k})^2] \|\rho_k - h_k^{i_k}\|^2 \leq \Xi_k - \Xi_{k+1} + \gamma_k R_3. \quad (33)$$

□

Case 21. Assume that there exists an integer $N \in \mathbb{N}$ such that $\Xi_{k+1} \leq \Xi_k$ for all $k \geq N$. This together with the boundedness of $\{\Xi_k\}$, it is convergent. Since $\lim_{k \rightarrow \infty} \gamma_k = 0$ and using Assumptions 13 and 14, and by (33),

$$\lim_{k \rightarrow \infty} \|\rho_k - h_k^{i_k}\| = \lim_{k \rightarrow \infty} \|S_{i_k} j_k^{i_k} - j_k^{i_k}\| = 0. \quad (34)$$

This combined with (16) yields that for all $i \in [K]$,

$$\begin{aligned} \|v_{k+1} - \rho_k\| &\leq \|v_{k+1} - j_k^{i_k}\| + \|j_k^{i_k} - \rho_k\| \\ &\leq (1 - \alpha_k^{i_k}) \|S_{i_k} j_k^{i_k} - j_k^{i_k}\| + (1 + \bar{\tau}_{i_k} \mathcal{L}_{i_k}) \|\rho_k - h_k^{i_k}\| \longrightarrow 0 \text{ as } k \longrightarrow \infty. \end{aligned} \quad (35)$$

This can be deduced from the definition of v_{k+1} that

$$\lim_{k \rightarrow \infty} \|\rho_k - u_k^i\| = 0, \quad (36)$$

for all $i \in [K]$. Using (15) again, we have

$$\begin{aligned} (1 - \alpha_k^i)(\alpha_k^i - \mu_i) \|S_i j_k^i - j_k^i\|^2 + [1 - (\bar{\tau}_i \mathcal{L}_i)^2] \|\rho_k - h_k^i\|^2 \leq \|\rho_k - v\|^2 - \|u_k^i - v\|^2 \\ \leq R_4 \|\rho_k - u_k^i\|, \end{aligned} \quad (37)$$

for all $i \in [K]$ and for some $R_4 > 0$. From the combination of this with (35) using Assumptions 13 and 14, we can derive that for all $i \in [K]$,

$$\lim_{k \rightarrow \infty} \|\rho_k - h_k^i\| = \lim_{k \rightarrow \infty} \|S_i j_k^i - j_k^i\| = 0. \quad (38)$$

From the definition of ρ_k , the inequality (27) and $\lim_{k \rightarrow \infty} \theta_k = 0$, we have

$$\begin{aligned} \|\rho_k - v_k\| &\leq \theta_k \|\Phi(v_k) - v_k\| + \xi_k \|v_k - v_{k-1}\|, \\ &\leq \theta_k (\|\Phi(v_k) - v_k\| + R_1) \longrightarrow 0 \text{ as } n \longrightarrow \infty. \end{aligned} \quad (39)$$

This together with (35) implies that

$$\lim_{k \rightarrow \infty} \|v_{k+1} - v_k\| = 0. \quad (40)$$

Moreover, because $\{v_k\}$ is bounded, there is $\bar{r} \in \mathcal{R}$ such that $v_{k_m} \rightarrow \bar{r}$ as $m \rightarrow \infty$ for some subsequence $\{v_{k_m}\}$ of $\{v_k\}$. From (39), we get $\rho_{k_m} \rightarrow \bar{r}$ as $m \rightarrow \infty$. Then using (38) with

Lemma 19 implies that $\bar{r} \in \Psi$. By (30), it is easy to demonstrate that

$$\limsup_{k \rightarrow \infty} \langle \Phi(v) - v, v_k - v \rangle = \lim_{m \rightarrow \infty} \langle \Phi(v) - v, v_{k_m} - v \rangle = \langle \Phi(v) - v, \bar{r} - v \rangle \leq 0. \quad (41)$$

Thus, we have by combining this with (40) that

$$\limsup_{k \rightarrow \infty} \langle \Phi(v) - v, v_{k+1} - v \rangle \leq \limsup_{k \rightarrow \infty} \langle \Phi(v) - v, v_{k+1} - v_k \rangle + \limsup_{k \rightarrow \infty} \langle \Phi(v) - v, v_k - v \rangle \leq 0. \quad (42)$$

Hence, from the assumption on Φ , (6), (7) and (29), we obtain

$$\begin{aligned} \Xi_{k+1} &\leq \|\rho_k - v\|^2 \\ &= \|\theta_k (\Phi(v_k) - \Phi(v)) + (1 - \theta_k)(v_k - v) + \xi_k (v_k - v_{k-1}) + \theta_k (\Phi(v) - v)\|^2 \\ &\leq \|\theta_k (\Phi(v_k) - \Phi(v)) + (1 - \theta_k)(v_k - v)\|^2 + 2\langle \xi_k (v_k - v_{k-1}) + \theta_k (\Phi(v) - v), v_{k+1} - v \rangle \\ &\leq \theta_k \|\Phi(v_k) - \Phi(v)\|^2 + (1 - \theta_k) \Xi_k + 2\xi_k \langle v_k - v_{k-1}, v_{k+1} - v \rangle + 2\theta_k \langle \Phi(v) - v, v_{k+1} - v \rangle \\ &\leq \theta_k \rho^2 \Xi_k + (1 - \theta_k) \Xi_k + 2\xi_k \|v_k - v_{k-1}\| \|v_{k+1} - v\| + 2\theta_k \langle \Phi(v) - v, v_{k+1} - v \rangle \\ &\leq \theta_k \rho \Xi_k + (1 - \theta_k) \Xi_k + 2\theta_k \cdot \frac{\xi_k}{\theta_k} \|v_k - v_{k-1}\| \|v_{k+1} - v\| + 2\theta_k \langle \Phi(v) - v, v_{k+1} - v \rangle \\ &\leq (1 - \gamma_k) \Xi_k + \gamma_k \left[R_5 \frac{\xi_k}{\theta_k} \|v_k - v_{k-1}\| + \frac{2}{1 - \rho} \langle \Phi(v) - v, v_{k+1} - v \rangle \right], \end{aligned} \quad (43)$$

for some $R_5 > 0$. As a consequence of applying this to the inequality (42) with Lemma 7, it can be inferred that $\lim_{k \rightarrow \infty} \Xi_k = 0$.

Case 22. We can find a subsequence $\{\Xi_{k_q}\}$ of $\{\Xi_k\}$ such that $\Xi_{k_q} < \Xi_{k_q+1}$ for all $q \in \mathbb{N}$. The inequality $\Xi_{\psi(k)} \leq \Xi_{\psi(k)+1}$ is derived by applying Lemma 8, where $\psi: \mathbb{N} \rightarrow \mathbb{N}$ is defined by (12), and $k \geq k^*$ for some $k^* \in \mathbb{N}$. By similar arguments as in Case 21, we obtain that

$$\lim_{k \rightarrow \infty} \|\rho_{\psi(k)} - h_{\psi(k)}^i\| = \lim_{k \rightarrow \infty} \|S_i j_{\psi(k)}^i - j_{\psi(k)}^i\| = 0, \quad (44)$$

for all $i \in [K]$ and

$$\limsup_{k \rightarrow \infty} \langle \Phi(v) - v, v_{\psi(k)+1} - v \rangle \leq 0. \quad (45)$$

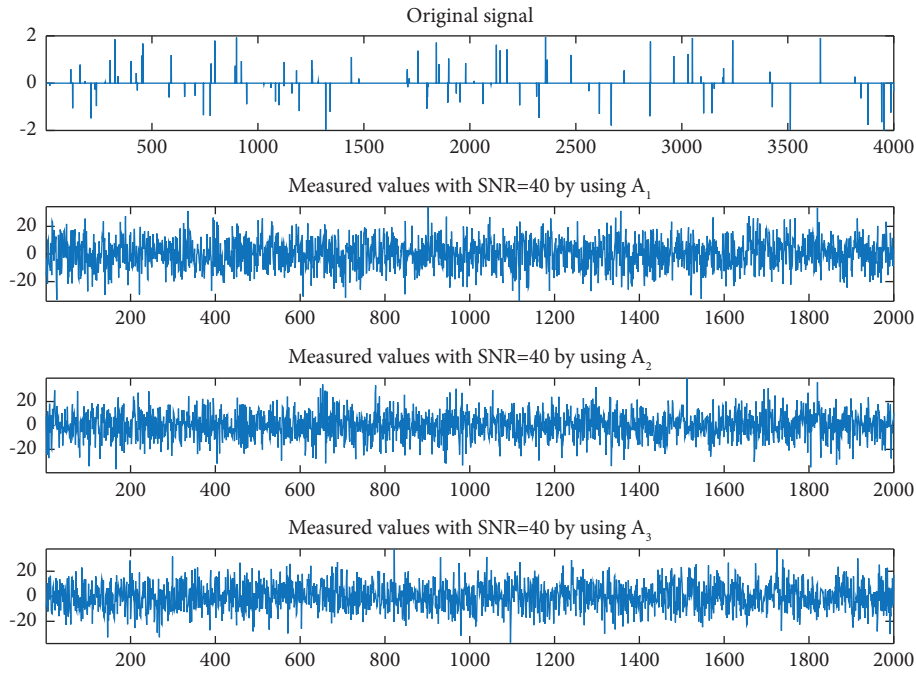
Finally, from $\Xi_{\psi(k)} \leq \Xi_{\psi(k)+1}$ and by (43), for all $k \geq k^*$, we obtain

$$\Xi_{\psi(k)+1} \leq (1 - \gamma_{\psi(k)}) \Xi_{\psi(k)+1} + \gamma_{\psi(k)} \left[R_5 \frac{\xi_{\psi(k)}}{\theta_{\psi(k)}} \|v_{\psi(k)} - v_{\psi(k)-1}\| + \frac{2}{1 - \rho} \langle \Phi(v) - v, v_{\psi(k)+1} - v \rangle \right]. \quad (46)$$

Some simple calculations yield

TABLE 1: Numerical comparison of four algorithms.

		m nonzero elements		
		$m = 100$	$m = 200$	$m = 300$
Algorithm 2.2	Number of iterations	1183	1271	1326
	CPU time (s)	10.0271	10.2887	10.7556
Algorithm 3	Number of iterations	381	433	481
	CPU time (s)	6.3097	6.9989	7.5401
Algorithm 1	Number of iterations	159	180	198
	CPU time (s)	3.9039	4.1992	4.5897
Algorithm 2	Number of iterations	169	193	212
	CPU time (s)	4.1950	4.5258	4.9377

FIGURE 1: From top to bottom: the original signal and the measurement by using A_1 , A_2 , and A_3 , respectively, with $m = 100$.

$$\Xi_{\psi(k)+1} \leq R_5 \frac{\xi_{\psi(k)}}{\theta_{\psi(k)}} \|v_{\psi(k)} - v_{\psi(k)-1}\| + \frac{2}{1-\rho} \langle \Phi(v) - v, v_{\psi(k)+1} - v \rangle. \quad (47)$$

This implies that $\limsup_{k \rightarrow \infty} \Xi_{\psi(k)+1} \leq 0$. Thus, $\lim_{k \rightarrow \infty} \Xi_{\psi(k)+1} = 0$. In addition, by Lemma 8,

$$\lim_{k \rightarrow \infty} \Xi_k \leq \lim_{k \rightarrow \infty} \Xi_{\psi(k)+1} = 0. \quad (48)$$

Therefore, it can be concluded that $v_k \rightarrow v$ as $k \rightarrow \infty$.

Theorem 23. *Assume that Assumptions 9–16 are satisfied. Then, the sequence $\{v_k\}$ generated by Algorithm 2 converges strongly to $v := (P_\Psi \circ \Phi)v$.*

Proof. Employing the same methodology as in the proof of ([48], Lemma 3.1.), we conclude that $\{\tau_k^i\} \subset [\min\{\tau_1^i, \lambda_i/\mathcal{L}_i\}, \tau_1^i] \subset (0, 1/\mathcal{L}_i)$ for all $i \in [K]$, that

is, Assumption 14 holds. The rest is similar to the proof of Theorem 20. \square

4. Application to Signal Recovery Problem

Signal recovery is a fundamental challenge in diverse scientific and engineering domains, and recent developments in signal recovery algorithms have resulted in substantial enhancements in the accuracy and efficacy of signal processing applications. Efficient signal recovery techniques are critical for numerous tasks, such as image and audio analysis, data compression, and communication systems. Consequently, sustained research and development efforts aimed at advancing signal recovery algorithms are

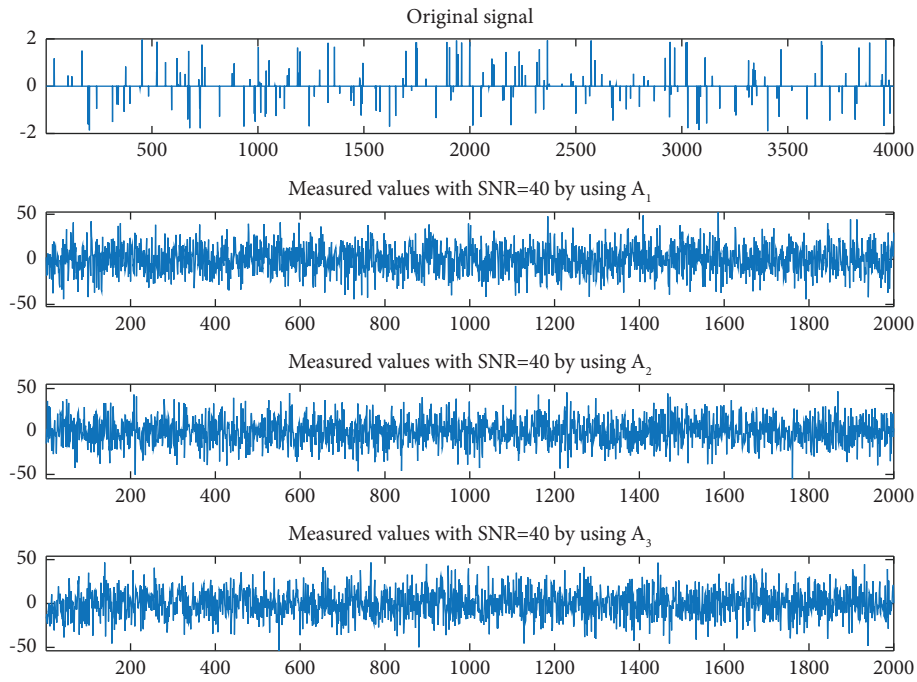


FIGURE 2: From top to bottom: the original signal and the measurement by using A_1 , A_2 , and A_3 , respectively, with $m = 200$.

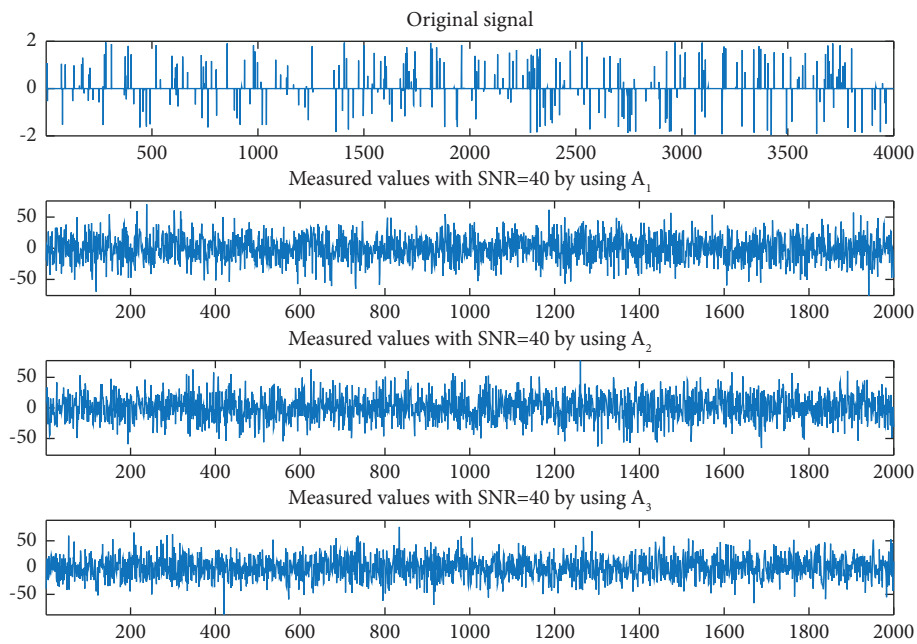


FIGURE 3: From top to bottom: the original signal and the measurement by using A_1 , A_2 , and A_3 , respectively, with $m = 300$.

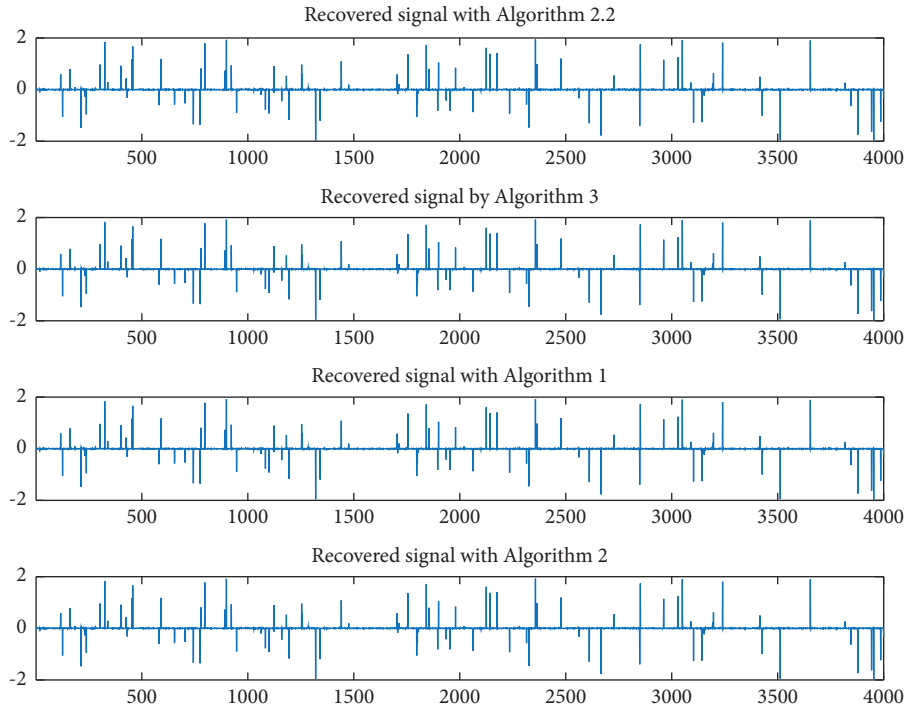


FIGURE 4: From top to bottom: the reconstructed signals by four algorithms for $m = 100$.

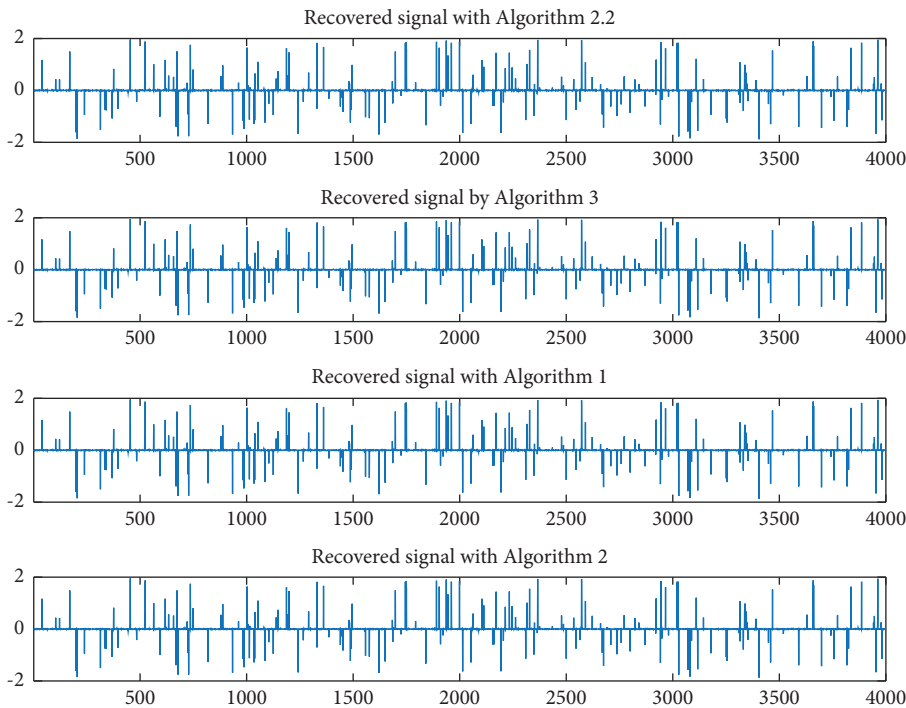


FIGURE 5: From top to bottom: the reconstructed signals by four algorithms for $m = 200$.

imperative to further enhance the performance and capabilities of these applications.

The signal recovery problem involving diverse blurring filters can be mathematically expressed as follows:

$$b_i = A_i x + \varepsilon_i, \tag{49}$$

where $b_i \in \mathbb{R}^M$ is the observed signal with noise ε_i , $x \in \mathbb{R}^N$ is the original signal and $A_i \in \mathbb{R}^{M \times N}$ ($M < N$) is filter matrix

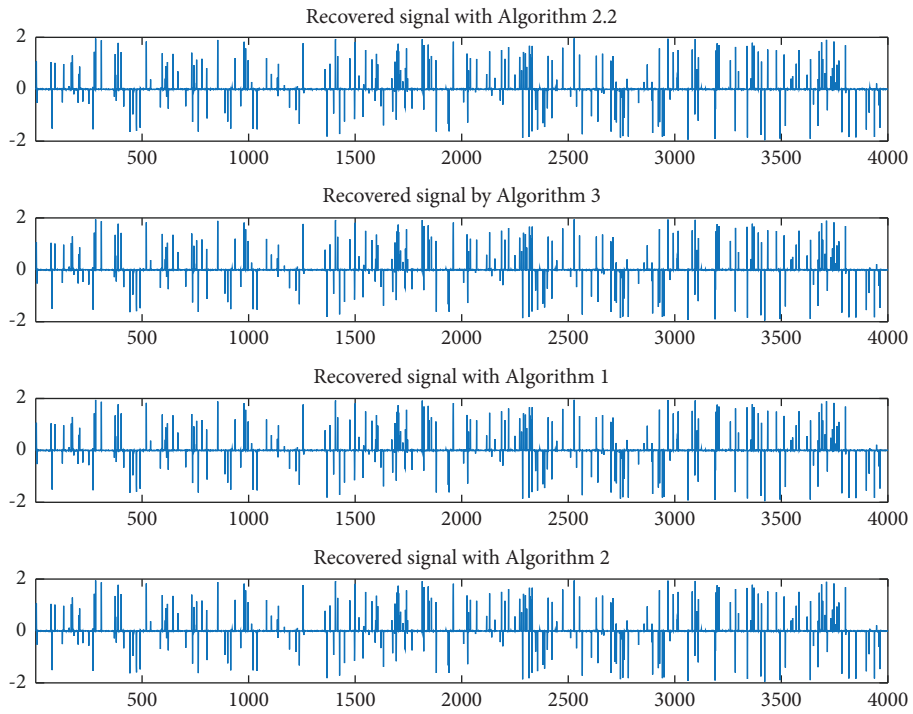


FIGURE 6: From top to bottom: the reconstructed signals by four algorithms for $m = 300$.

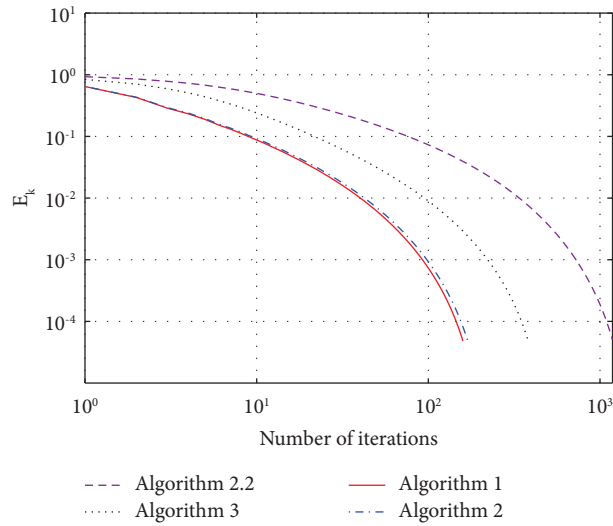


FIGURE 7: Plots of E_k over iter when $m = 100$.

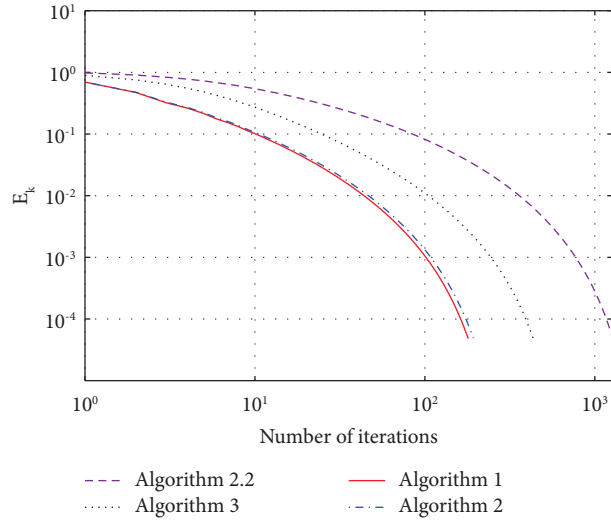


FIGURE 8: Plots of E_k over iter when $m = 200$.

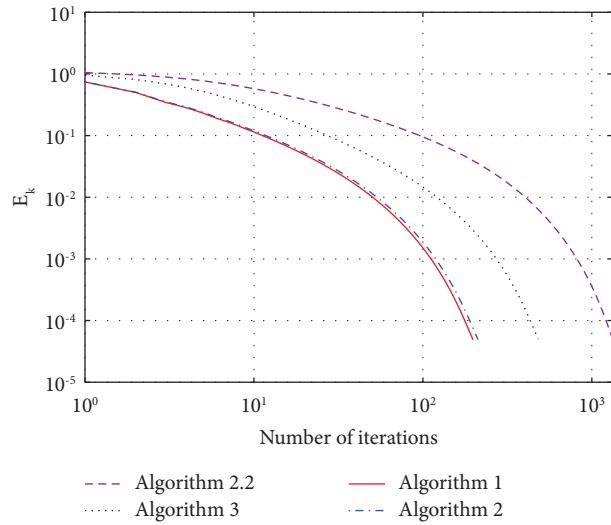


FIGURE 9: Plots of E_k over iter when $m = 300$.

TABLE 2: Numerical results of Algorithms 1.

Inputs		m nonzero elements		
		$m = 50$	$m = 100$	$m = 150$
A_1	Number of iterations	2373	3143	4474
	CPU time (s)	3.4571	4.4129	6.2303
A_2	Number of iterations	2328	3407	4297
	CPU time (s)	3.1495	4.8879	5.8837
A_3	Number of iterations	2334	3162	4316
	CPU time (s)	3.1203	4.2016	6.1732
A_1, A_2	Number of iterations	581	564	762
	CPU time (s)	2.0524	1.9764	2.9730
A_1, A_3	Number of iterations	548	589	685
	CPU time (s)	2.8591	2.0762	3.5921
A_2, A_3	Number of iterations	598	629	644
	CPU time (s)	2.3680	2.1654	2.9194
A_1, A_2, A_3	Number of iterations	138	145	154
	CPU time (s)	0.8413	0.7845	0.8708

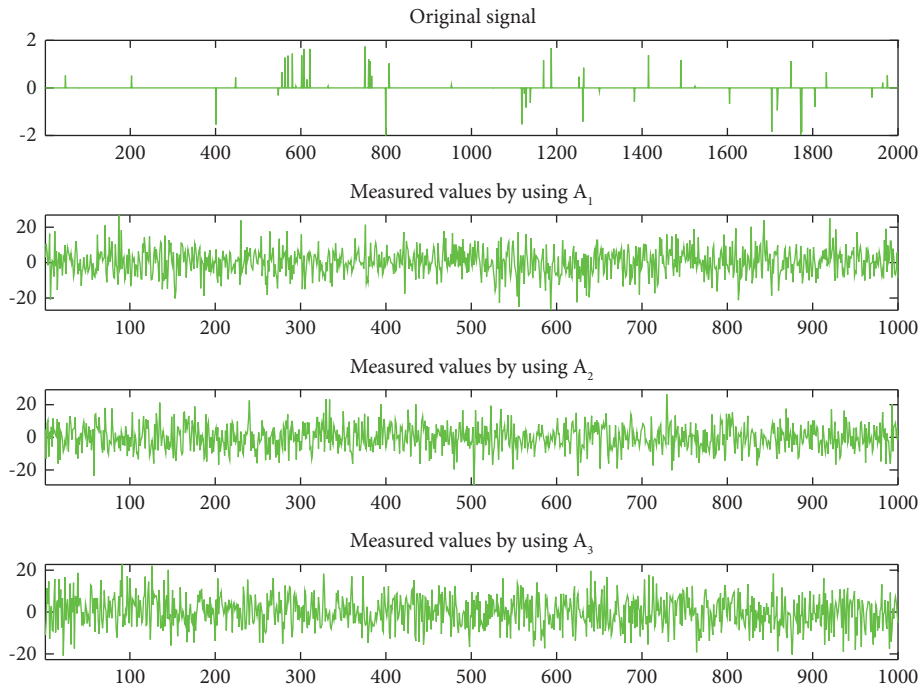


FIGURE 10: From top to bottom: the original signal and the measurement by using A_1 , A_2 , and A_3 , respectively, with $m = 50$.

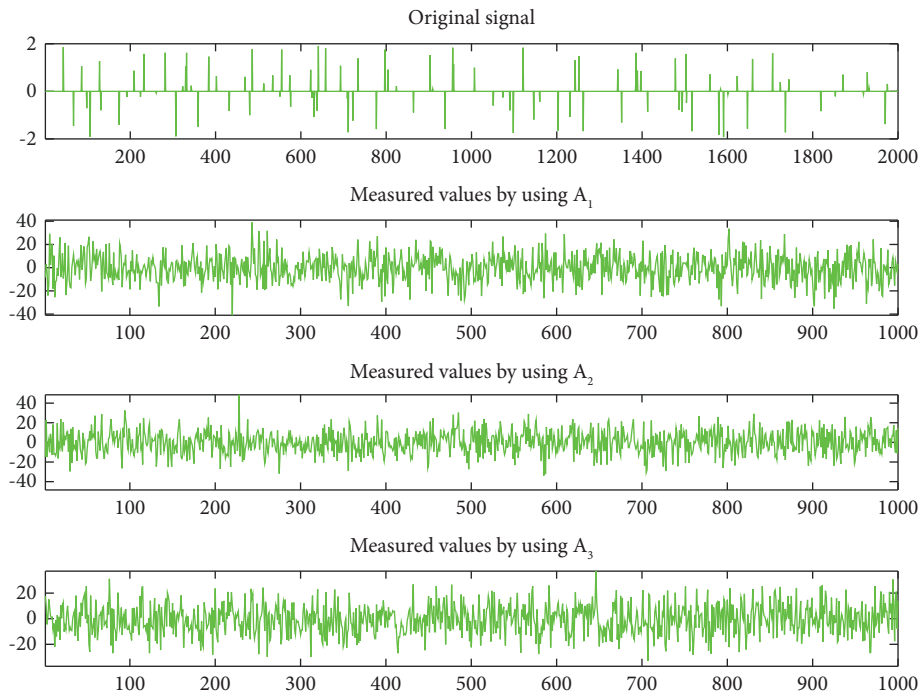


FIGURE 11: From top to bottom: the original signal and the measurement by using A_1 , A_2 , and A_3 , respectively, with $m = 100$.

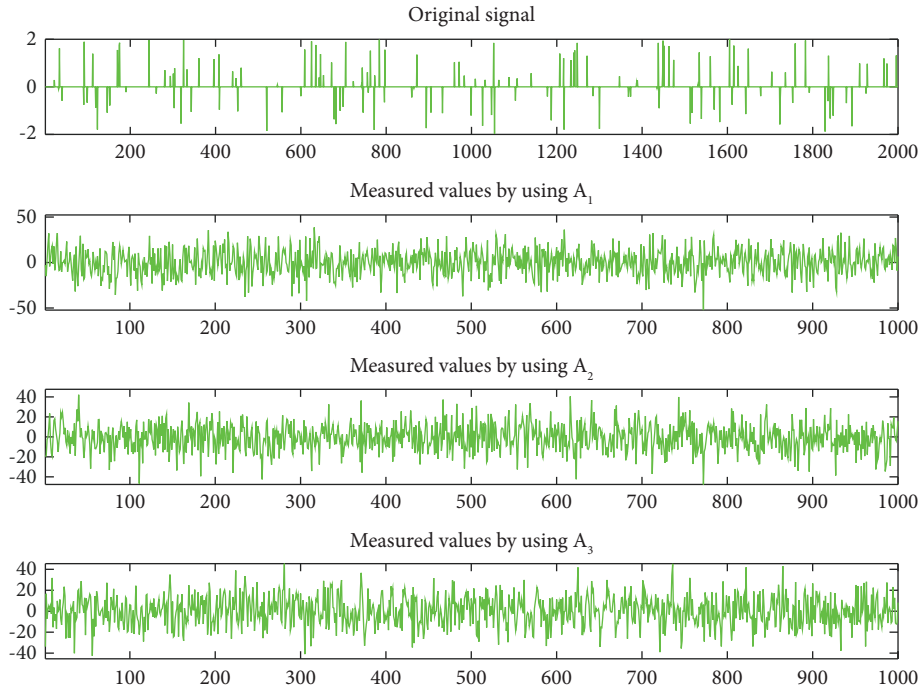


FIGURE 12: From top to bottom: the original signal and the measurement by using A_1 , A_2 , and A_3 , respectively, with $m = 150$.

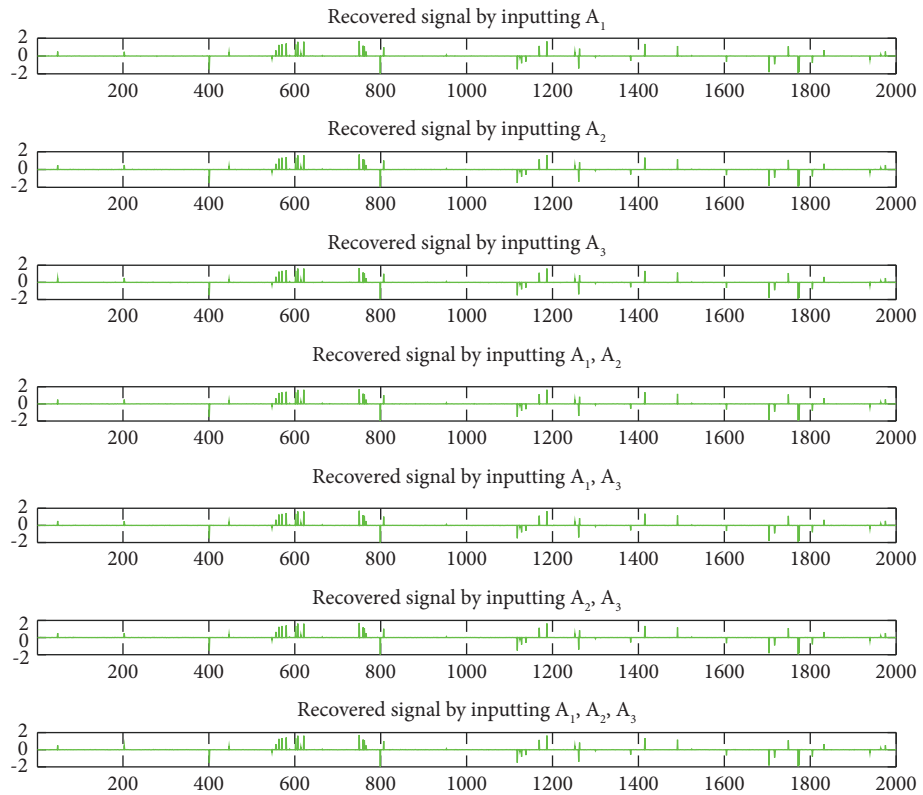


FIGURE 13: From top to bottom: the reconstructed signals by using each input for $m = 50$.

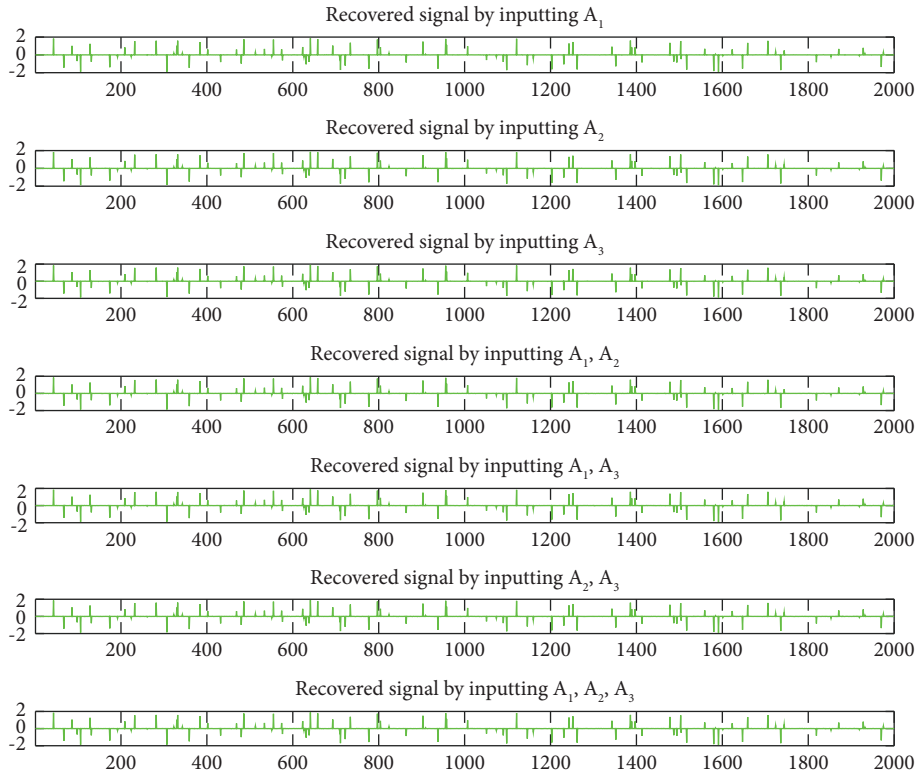


FIGURE 14: From top to bottom: the reconstructed signals by using each input for $m = 100$.

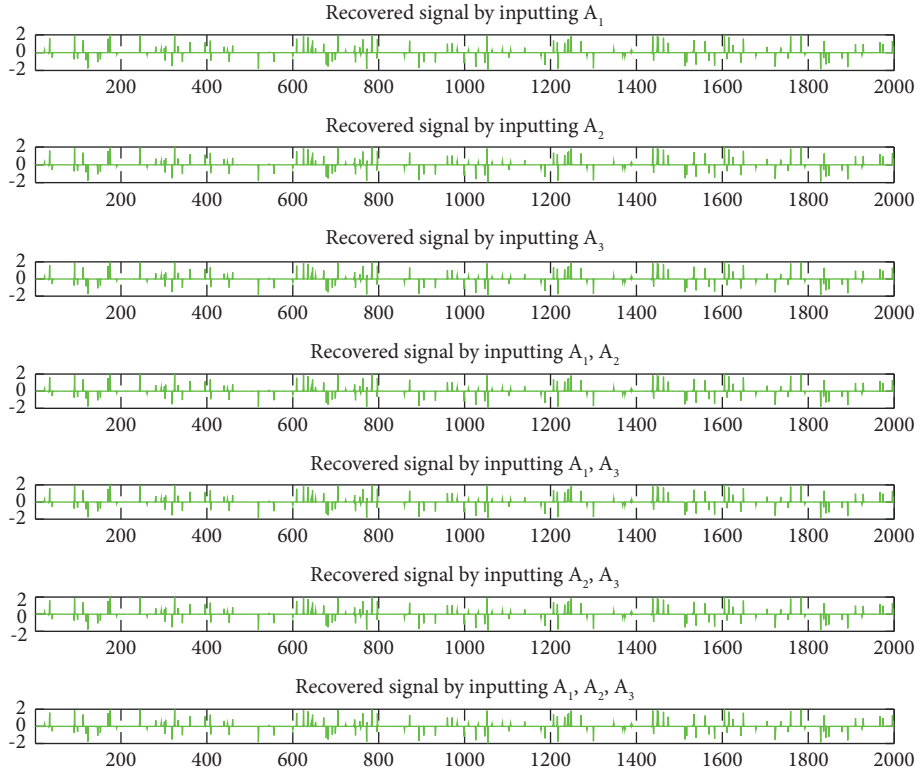


FIGURE 15: From top to bottom: the reconstructed signals by using each input for $m = 150$.

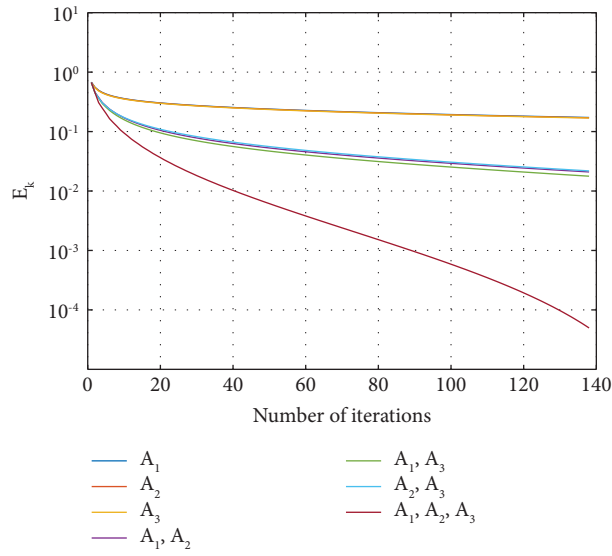


FIGURE 16: Plots of E_k over iter when $m = 50$.

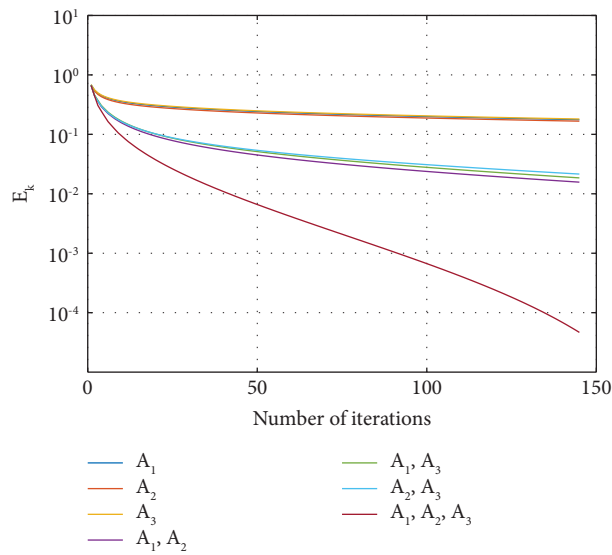


FIGURE 17: Plots of E_k over iter when $m = 100$.

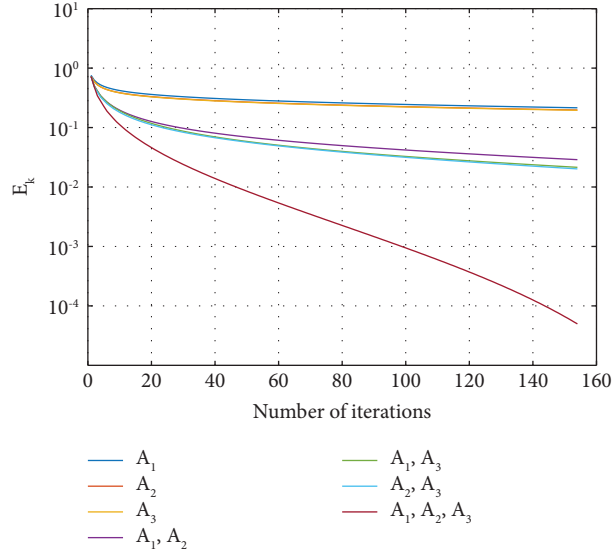


FIGURE 18: Plots of E_k over iter when $m = 150$.

for all $i \in [K]$. Subsequently, we direct our attention toward the following problem:

$$\begin{aligned} & \min_{x \in \mathbb{R}^N} \frac{1}{2} \|A_1 x - b_1\|_2^2 + \|x\|_1, \\ & \min_{x \in \mathbb{R}^N} \frac{1}{2} \|A_2 x - b_2\|_2^2 + \|x\|_1, \\ & \min_{x \in \mathbb{R}^N} \frac{1}{2} \|A_3 x - b_3\|_2^2 + \|x\|_1, \\ & \vdots \\ & \min_{x \in \mathbb{R}^N} \frac{1}{2} \|A_K x - b_K\|_2^2 + \|x\|_1, \end{aligned} \quad (50)$$

for all $i \in [K]$. According to Proposition 3.1 (iii) presented in [49], the problem at hand can be recast as problem (2) through the following settings: $\mathcal{H} = \mathbb{R}^N$, $S_i(\cdot) = \text{prox}_{\zeta_i \|\cdot\|_1}(I - \zeta_i \nabla h_i)(\cdot)$, $G_i(\cdot) = \partial(\|\cdot\|_1)$ and $F_i = \nabla h_i$, where $\zeta_i > 0$, $h_i(\cdot) = 1/2 \|A_i(\cdot) - b_i\|_2^2$ for all $i \in [K]$. It is known that S_i is nonexpansive mapping for $\zeta_i \in (0, 2/\|A_i\|_2^2)$ and hence 0-demicontractive. Besides, G_i is maximal monotone mapping, and F_i is monotone and $\|A_i\|_2^2$ -Lipschitz continuous mapping.

In this part, we perform two numerical experiments to present the computational efficiency of Algorithms 1 and 2 for signal recovery problems consisting of various blurring filters. All computations were performed using Matlab R2021a on an iMac equipped with an Apple M1 chip and 16 GB of RAM. Experiment (***) During the first experiment, we provide the numerical comparison of Algorithms 1 and 2 with Algorithm of Corollary 2.2 in [31] (Algorithm 2.2) and Algorithm 3 in [50]. Select the signal size to be $N = 4000$ and $M = 2000$. Set the original signal x is generated by the uniform distribution in $[-2, 2]$ with m nonzero elements

and A_i be the Gaussian matrix generated by command `randn(M, N)`. Let the observation b_i be generated by white Gaussian noise with signal-to-noise ratio $\text{SNR} = 40$, the initial points be the vectors generated randomly and $\zeta_i = 1/\|A_i\|_2^2$ for all $i \in \{1, 2, 3\}$. Measuring the accuracy of the restoration using the mean-squared error, which is defined as: $E_k = 1/N \|v_k - x\|_2^2 < 5 \times 10^{-5}$. The control parameters are defined in the following manner:

- (i) Algorithm 2.2: $\alpha_k^n = 0.5$;
- (ii) Algorithm 3: $\lambda_i = 0.5$, $\varphi(\cdot) = 0.9(\cdot)$, $\gamma_1^i = 9/10 \|A_i\|_2^2$, $a_k = 1/k + 1$, $b_k = 99k/100(k + 1)$ and $\xi_k = \begin{cases} \min\{1/(k+1)^{1.1} \max\{\|u_k - u_{k-1}\|_2, \|u_k - u_{k-1}\|_2^2\}, 0.25\} & \text{if } u_k \neq u_{k-1}; \\ 0.25 & \text{otherwise;} \end{cases}$
- (iii) Algorithm 1: $\alpha_k^i = 0.25$, $\Phi(\cdot) = 0.9(\cdot)$, $\tau_1^i = 9/10 \|A_i\|_2^2$, $\theta_k = 1/k + 1$ and $\xi_k = \begin{cases} \min\{1/(k+1)^{1.1} \max\{\|v_k - v_{k-1}\|_2, \|v_k - v_{k-1}\|_2^2\}, 0.25\} & \text{if } v_k \neq v_{k-1}; \\ 0.25 & \text{otherwise;} \end{cases}$
- (iv) Algorithm 2: $\lambda_i = 0.5$, $\alpha_k^i = 0.25$, $\Phi(\cdot) = 0.9(\cdot)$, $\tau_1^i = 9/10 \|A_i\|_2^2$, $\theta_k = 1/k + 1$ and $\xi_k = \begin{cases} \min\{1/(k+1)^{1.1} \max\{\|v_k - v_{k-1}\|_2, \|v_k - v_{k-1}\|_2^2\}, 0.25\} & \text{if } v_k \neq v_{k-1}; \\ 0.25 & \text{otherwise;} \end{cases}$

The following results are shown.

The numerical results of Experiment (***) clearly demonstrate that both proposed algorithms are more effective than the two previous algorithms, as indicated in Table 1 and Figures 1–9.

Experiment 24. In the second experiment, we present the numerical results obtained via Algorithm 1 for solving problem (4.1) with multiple inputs A_i . The signal size is set to be $N = 2000$ and $M = 1000$, with the original signal x being generated via a uniform distribution over the interval $[-2, 2]$, featuring m nonzero elements. The matrices A_i are Gaussian matrices generated using the command `randn(M, N)`. For $i \in \{1, 2, 3\}$, the observations b_i are generated via the addition of white Gaussian noise ε_i with variance σ_i^2 , with initial points being randomly generated

and $\zeta_i = 1/\|A_i\|_2^2$. Measuring the accuracy of the restoration using the mean-squared error, which is defined as follows: $E_k = 1/N\|v_k - x\|_2^2 < 5 \times 10^{-5}$. For Algorithm 1, let $\sigma_i = 0.01$ (i), $\alpha_k^i = 0.25$, $\Phi(\cdot) = 0.9(\cdot)$, $\tau_k^i = 9/10\|A_i\|_2^2$, $\theta_k = 1/k + 1$ and $\xi_k = \begin{cases} \min\{1/(k+1)^{1.1} \max\{\|v_k - v_{k-1}\|_2, \|v_k - v_{k-1}\|_2^2\}, 0.25\} & \text{if } v_k \neq v_{k-1}; \\ 0.25 & \text{otherwise;} \end{cases}$ The ensuing section depicts the results.

Based on the numerical results obtained from Experiment 24, it is evident that incorporating all three Gaussian matrices (A_1, A_2 , and A_3) into Algorithm 1 leads to more effective outcomes in terms of time and number of iterations, as compared to the usage of only one or two of the matrices. These results are presented in Table 2 and Figures 10–18.

5. Conclusions

In this research, we obtain strong convergence results for common variational inclusion and common fixed point problems using two new parallel methods. Our results extend and generalize several previously published findings, and the numerical results indicate that our suggested approaches to the signal recovery problem including multiple blurring filters outperform the two preceding approaches.

Data Availability

The data used to support the findings of the study are available from the corresponding author upon request.

Conflicts of Interest

The authors declare that they have no conflicts of interest.

Acknowledgments

This research project was partially supported by Suan Dusit University Lampang Center, King Mongkut's University of Technology Thonburi, Faculty of Science, Chiang Mai University, and Chiang Mai University.

References

- [1] A. Beck and M. Teboulle, "A fast iterative shrinkage-thresholding algorithm for linear inverse problems," *SIAM Journal on Imaging Sciences*, vol. 2, no. 1, pp. 183–202, 2009.
- [2] Y. Shehu and P. Cholamjiak, "Iterative method with inertial for variational inequalities in Hilbert spaces," *Calcolo*, vol. 56, no. 1, p. 4, 2019.
- [3] S. Suantai, S. Kesornprom, and P. Cholamjiak, "A new hybrid CQ algorithm for the split feasibility problem in Hilbert spaces and its applications to compressed sensing," *Mathematics*, vol. 7, no. 9, p. 789, 2019.
- [4] R. Suparatulorn, P. Charoensawan, and K. Pochinapan, "Inertial self-adaptive algorithm for solving split feasible problems with applications to image restoration," *Mathematical Methods in the Applied Sciences*, vol. 42, no. 18, pp. 7268–7284, 2019.
- [5] S. Kesornprom, N. Pholasa, and P. Cholamjiak, "On the convergence analysis of the gradient-CQ algorithms for the split feasibility problem," *Numerical Algorithms*, vol. 84, no. 3, pp. 997–1017, 2020.
- [6] P. Peeyada, R. Suparatulorn, and W. Cholamjiak, "An inertial Mann forward-backward splitting algorithm of variational inclusion problems and its applications," *Chaos, Solitons & Fractals*, vol. 158, Article ID 112048, 2022.
- [7] S. Kesornprom and P. Cholamjiak, "A modified inertial proximal gradient method for minimization problems and applications," *AIMS Mathematics*, vol. 7, no. 5, pp. 8147–8161, 2022.
- [8] P. L. Lions and B. Mercier, "Splitting algorithms for the sum of two nonlinear operators," *SIAM Journal on Numerical Analysis*, vol. 16, no. 6, pp. 964–979, 1979.
- [9] G. B. Passty, "Ergodic convergence to a zero of the sum of monotone operators in Hilbert space," *Journal of Mathematical Analysis and Applications*, vol. 72, no. 2, pp. 383–390, 1979.
- [10] G. H.-G. Chen and R. T. Rockafellar, "Convergence rates in forward-backward splitting," *SIAM Journal on Optimization*, vol. 7, no. 2, pp. 421–444, 1997.
- [11] P. Tseng, "A modified forward-backward splitting method for maximal monotone mappings," *SIAM Journal on Control and Optimization*, vol. 38, no. 2, pp. 431–446, 2000.
- [12] B. Polyak, "Some methods of speeding up the convergence of iteration methods," *USSR Computational Mathematics and Mathematical Physics*, vol. 4, no. 5, pp. 791–817, 1964.
- [13] A. Padcharoen, D. Kitkuan, W. Kumam, and P. Kumam, "Tseng methods with inertial for solving inclusion problems and application to image deblurring and image recovery problems," *Computational and Mathematical Methods*, vol. 3, no. 3, Article ID e1088, 2021.
- [14] D. A. Lorenz and T. Pock, "An inertial forward-backward algorithm for monotone inclusions," *Journal of Mathematical Imaging and Vision*, vol. 51, no. 2, pp. 311–325, 2015.
- [15] S. Kesornprom and P. Cholamjiak, "Proximal type algorithms involving linesearch and inertial technique for split variational inclusion problem in hilbert spaces with applications," *Optimization*, vol. 68, no. 12, pp. 2369–2395, 2019.
- [16] S. Suantai, S. Kesornprom, and P. Cholamjiak, "Modified proximal algorithms for finding solutions of the split variational inclusions," *Mathematics*, vol. 7, no. 8, p. 708, 2019.
- [17] J. Abubakar, P. Kumam, A. I. Garba, M. S. Abdullahi, A. H. Ibrahim, and K. Sitthithakerngkiet, "An inertial iterative scheme for solving variational inclusion with application to Nash-Cournot equilibrium and image restoration problems," *Carpathian Journal of Mathematics*, vol. 37, no. 3, pp. 361–380, 2021.
- [18] W. Cholamjiak, P. Cholamjiak, and S. Suantai, "An inertial forward-backward splitting method for solving inclusion problems in Hilbert spaces," *Journal of Fixed Point Theory and Applications*, vol. 20, no. 1, p. 42, 2018.

- [19] P. Cholamjiak, D. Van Hieu, and Y. J. Cho, "Relaxed forward-backward splitting methods for solving variational inclusions and applications," *Journal of Scientific Computing*, vol. 88, no. 3, p. 85, 2021.
- [20] A. Gibali and D. V. Thong, "Tseng type methods for solving inclusion problems and its applications," *Calcolo*, vol. 55, pp. 49–54, 2018.
- [21] A. Taiwo, O. T. Mewomo, and A. Gibali, "A simple strong convergent method for solving split common fixed point problems," *Journal of Nonlinear and Variational Analysis*, vol. 5, no. 5, pp. 777–793, 2021.
- [22] C. Zong and Y. Tang, "Dual three-operator splitting algorithms for solving composite monotone inclusion with applications to convex minimization," *Journal of Applied and Numerical Optimization*, vol. 3, no. 3, pp. 533–554, 2021.
- [23] J. Xiao and Y. Wang, "A viscosity method with inertial effects for split common fixed point problems of demicontractive mappings," *Journal of Nonlinear Functional Analysis*, vol. 2022, 2022.
- [24] X. Zhao, J. C. Yao, and Y. Yao, "A proximal algorithm for solving split monotone variational inclusions," *University Politehnica of Bucharest Scientific Bulletin, Series A: Applied Mathematics and Physics*, vol. 82, no. 3, pp. 43–52, 2020.
- [25] R. H. Haghi and N. Bakhshi, "Some coupled fixed point results without mixed monotone property," *Journal of Advanced Mathematical Studies*, vol. 15, no. 4, pp. 456–463, 2022.
- [26] D. W. Peaceman and H. H. Rachford Jr, "The numerical solution of parabolic and elliptic differential equations," *Journal of the Society for Industrial and Applied Mathematics*, vol. 3, no. 1, pp. 28–41, 1955.
- [27] J. Douglas and H. H. Rachford, "On the numerical solution of heat conduction problems in two and three space variables," *Transactions of the American Mathematical Society*, vol. 82, no. 2, pp. 421–439, 1956.
- [28] G. Li and T. K. Pong, "Douglas-Rachford splitting for non-convex optimization with application to non-convex feasibility problems," *Mathematical Programming*, vol. 159, no. 1–2, pp. 371–401, 2016.
- [29] M. N. Dao and H. M. Phan, "Adaptive Douglas-Rachford splitting algorithm for the sum of two operators," *SIAM Journal on Optimization*, vol. 29, no. 4, pp. 2697–2724, 2019.
- [30] C. K. Sim, "Convergence rates for the relaxed Peaceman-Rachford splitting method on a monotone inclusion problem," *Journal of Optimization Theory and Applications*, vol. 196, no. 1, pp. 298–323, 2023.
- [31] S. Suantai, K. Kankam, P. Cholamjiak, and W. Cholamjiak, "A parallel monotone hybrid algorithm for a finite family of G -nonexpansive mappings in Hilbert spaces endowed with a graph applicable in signal recovery," *Computational and Applied Mathematics*, vol. 40, no. 4, 2021.
- [32] R. Suparatulorn and K. Chaichana, "A strongly convergent algorithm for solving common variational inclusion with application to image recovery problems," *Applied Numerical Mathematics*, vol. 173, pp. 239–248, 2022.
- [33] S. S. Chang, C. F. Wen, and J. C. Yao, "Common zero point for a finite family of inclusion problems of accretive mappings in Banach spaces," *Optimization*, vol. 67, no. 8, pp. 1183–1196, 2018.
- [34] T. Mouktonglang, K. Poochinapan, and R. Suparatulorn, "A parallel method for common variational inclusion and common fixed point problems with applications," *Carpathian Journal of Mathematics*, vol. 39, no. 1, pp. 189–200, 2022.
- [35] P. K. Anh and D. Van Hieu, "Parallel and sequential hybrid methods for a finite family of asymptotically quasi ϕ -nonexpansive mappings ϕ -nonexpansive mappings," *Journal of Applied Mathematics and Computing*, vol. 48, no. 1–2, pp. 241–263, 2015.
- [36] W. Cholamjiak, S. A. Khan, D. Yambangwai, and K. R. Kazmi, "Strong convergence analysis of common variational inclusion problems involving an inertial parallel monotone hybrid method for a novel application to image restoration," *Revista de la Real Academia de Ciencias Exactas, Físicas y Naturales, Serie A. Matemáticas*, vol. 1142 pages, 2020.
- [37] M. Eslamian, "Strong convergence theorem for common zero points of inverse strongly monotone mappings and common fixed points of generalized demimetric mappings," *Optimization*, vol. 71, no. 14, pp. 4265–4287, 2021.
- [38] M. Eslamian and A. Kamandi, "A novel algorithm for approximating common solution of a system of monotone inclusion problems and common fixed point problem," *Journal of Industrial and Management Optimization*, vol. 19, no. 2, pp. 868–889, 2023.
- [39] S. Suantai, W. Cholamjiak, and P. Cholamjiak, "Strong convergence theorems of a finite family of quasi-nonexpansive and Lipschitz multi-valued mappings," *Afrika Matematika*, vol. 26, no. 3–4, pp. 345–355, 2015.
- [40] T. L. Hicks and J. D. Kubicek, "On the Mann iteration process in a Hilbert space," *Journal of Mathematical Analysis and Applications*, vol. 59, no. 3, pp. 498–504, 1977.
- [41] Ş. Mâruşter, "The solution by iteration of nonlinear equations in Hilbert spaces," *Proceedings of the American Mathematical Society*, vol. 63, no. 1, pp. 69–73, 1977.
- [42] H. Y. Zhou and X. L. Qin, *Fixed Points of Nonlinear Operators. Iterative Methods*, De Gruyter, Berlin, Germany, 2020.
- [43] H. Brézis, "Opérateurs Maximaux Monotones et Semigroupes de Contractions dans les Espaces de Hilbert," *Math. Studies 5*, North-Holland, Amsterdam, Netherlands, 1973.
- [44] H. H. Bauschke and P. L. Combettes, "Convex analysis and monotone operator theory in hilbert spaces," *CMS Books in Mathematics*, Springer, New York, NY, USA, 2011.
- [45] B. Tan, Z. Zhou, and S. Li, "Viscosity-type inertial extragradient algorithms for solving variational inequality problems and fixed point problems," *Journal of Applied Mathematics and Computing*, vol. 68, no. 2, pp. 1387–1411, 2022.
- [46] H. K. Xu, "Iterative algorithms for nonlinear operators," *Journal of the London Mathematical Society*, vol. 66, no. 1, pp. 240–256, 2002.
- [47] P. E. Maingé, "Strong convergence of projected subgradient methods for nonsmooth and nonstrictly convex minimization," *Set-Valued Analysis*, vol. 16, no. 7–8, pp. 899–912, 2008.
- [48] J. Yang and H. Liu, "Strong convergence result for solving monotone variational inequalities in Hilbert space," *Numerical Algorithms*, vol. 80, no. 3, pp. 741–752, 2019.
- [49] P. L. Combettes and V. R. Wajs, "Signal recovery by proximal forward-backward splitting," *Multiscale Modeling and Simulation*, vol. 4, pp. 1168–1200, 2005.
- [50] R. Suparatulorn, W. Cholamjiak, A. Gibali, and T. Mouktonglang, "A parallel Tseng's splitting method for solving common variational inclusion applied to signal recovery problems," *Advances in Difference Equations*, vol. 2021, no. 1, p. 492, 2021.